Dokuz Eylül Üniversitesi-Mühendislik Fakültesi
Fen ve Mühendislik Dergisi
Cilt 20, Sayı 60, Eylül, 2018

Dokuz Eylul University-Faculty of Engineering
Journal of Science and Engineering
Volume 20, Issue 60, September, 2018

DOI: 10.21205/deufmd. 2018206083

# Free Vibration and Torsional Buckling Analysis of E- Glass/Epoxy Composite Shafts with Polyamide-6,6 (PA 66) Nanofiber Interlayers

**Bertan BEYLERGİL**

Alanya Alaaddin Keykubat Üniversitesi, Mühendislik Fakültesi, Makine Mühendisliği Bölümü, 07425, Alanya. *(ORCID: 0000-0002-3204-6746)*

(Alınış / Received: 24.04.2018, Kabul / Accepted: 26.06.2018,
Online Yayınlanma / Published Online: 15.09.2018)

**Keywords**
composite shaft, PA 66 nanofibers, natural frequencies, torsional buckling

**Abstract:** In this study, the effects of polyamide-6,6 (PA 66) nanofibers on the free vibration and torsional buckling of four-layered E-glass/epoxy composite drive shaft were investigated numerically. The numerical analyses were carried out by using ANSYS 16.2 software package. Three different nanofiber areal weight densities (AWDs), 8, 10 and 12 g/m$^2$, were considered to reveal the relationship between the amount of nanofibers in the interlaminar region and natural frequencies/critical torsional buckling loads. The numerical results showed that the PA-66 nanofibers had a positive effect on natural frequencies and torsional buckling load of E-glass/epoxy composite shaft. The natural frequencies and buckling load of the composite shaft can be increased by about 10 % and 22% using PA 66 nanofibers as the secondary reinforcing material in the interlaminar region. The failure torque values were not significantly affected with the inclusion of PA 66 nanofibers in the interlaminar region.

# Arayüzeyinde Poliamid 6,6 (PA 66) Nanofiber Tabakalar Bulunan Cam Elyaf/Epoksi Kompozit Şaftların Serbest Titreşim ve Burulma Burkulması Analizi

**Anahtar kelimeler**
Kompozit şaft, PA 66 nanofiberler, Doğal frekanslar, Burulma burkulması

**Özet:** Bu çalışmada, PA 66 nanofiberlerin dört tabakalı cam elyaf/epoksi kompozit şaftın serbest titreşim ve burulma burkulmasına etkisi nümerik olarak incelenmiştir. Nümerik analizler ANSYS 16.2 sonlu elemanlar programı kullanılarak gerçekleştirilmiştir. Üç farklı nanofiber alansal yoğunluğu (8, 10 and 12 g/m$^2$) ele alınarak, nanofiber miktarının titreşim frekanslarına ve burulma burkulması yüküne etkileri ortaya çıkarılmıştır. Nümerik sonuçlara göre, PA 66 nanofiberlerin kompozit şaftın serbest titreşim frekanslarına ve burkulma yüküne sırasıyla %10 ve %22 oranında pozitif etkisi olduğu

gözlemlenmiştir. PA 66 nanofiberlerin kompozit şaftın burulma yüküne hasar etkisi önemli bir etkisi görülmemiştir.

*Sorumlu yazar: bertan.beylergil@alanya.edu.tr

## 1. Introduction

Fiber reinforced composites have been extensively used in many structural applications due to their unique advantages such as high strength and stiffness at low weight, good corrosion resistance and fatigue properties. However, they are prone to delamination failure during their service life. This failure mode may occur insidiously due to low-velocity impact events, manufacturing imperfections and sudden geometrical changes in structural details. It causes severe reductions in the in-plane stiffness and strength values which results in accelerated growth of damage and premature failure. Therefore, a number of techniques to improve delamination resistance of fiber reinforced composites were developed by the researchers over the years [1-3].

The use of thermoplastic electrospun nanofibers in the interlaminar region of composites is one of the most promising techniques due to some unique advantages such as improved delamination resistance (up to 3 times depending on the polymer type and nanofiber areal weight density) with uncompromised in-plane mechanical properties, no additional weight/thickness and unchanged resin viscosity [5-8]. The first commercial suppliers of electrospun nanofiber interlayers are on the market and the transition of these nano interlayers into commercial products has already started. The first real-life application of nanointerleaved composites can be seen in a carbon fiber/epoxy fishing rod manufactured by Kilwell Sports Ltd. The bending strength of these fishing rods was almost 100% higher than those of the old-fashioned ones [9].

Up to date, only one research by Garcia et al. [10] was dedicated to the effects of PA 66 nanointerlayers on the free vibration behavior of fiber reinforced composites. The authors showed that the nano-modified composites led to significant increase in the damping ratio and interlaminar strength compared to unmodified composites. Further research is needed to expand knowledge and understanding the effects of nanointerleaving technique for the other possible structural applications.

Fiber reinforced composites have shown to be an ideal replacement material for long, power drive shaft applications. However, delamination is a serious problem for rotating composite shafts. Most of the studies in the literature focused on the optimum design and analysis of composite drive shafts. Recently, multi-objective optimization (MOP) of a composite drive shaft was performed by Khalkhali et al. [11] considering three conflicting objectives; fundamental natural frequency, critical buckling torque and weight of the shaft. The design variables were ply material, ply thickness and fiber orientation. They obtained the optimum design parameters for higher natural frequency values, critical buckling loads with a minumum weight of structure. In another study by Talib et al. [12], numerical studies were carried out to design composite drive shafts composed of carbon and glass fibers within an epoxy matrix in terms of buckling load, load bearing capacity and natural frequency. Unlike the other studies in the literature, this study investigates the effects of PA 66 nanointerlayers on the free vibration and torsional buckling and failure loads of E-glass/epoxy composite drive shafts were investigated numerically. Numerical analyses were carried out by using ANSYS

16.2 software package. This study aims to make a unique contribution on this research gap and presents a new win-win solution to enhance the torsional buckling capacity as well as delamination resistance of existing composite drive shafts.

## 2. Finite element analysis

Finite element analyses of the composite drive shafts were carried out by using ANSYS Workbench with ACP module. Free vibration frequency values and torsional buckling loads of the reference and PA 66 nanointerlayered composite shafts were determined. The Tsai–Wu criterion was also used to judge the torsional stability of the composite shafts. Figure 1 shows the project schematic of ANSYS Workbench used for this study.

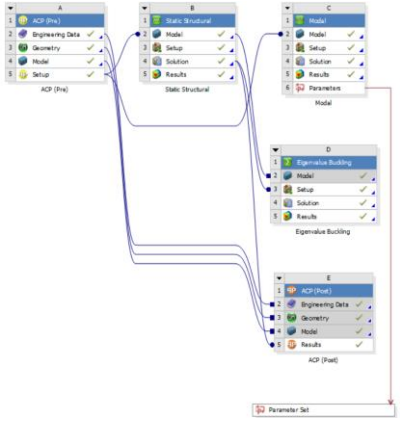

**Figure 1.** Project schematic of ANSYS Workbench used in this study

### 2.1. Numerical verification

In order to ensure the accuracy of the finite element model, firstly the FE model was verified against the results of published research by Khalkhali et al. [11]. The geometry and dimensions of the composite shafts used for the validation of the finite element method was shown in Figure 2.

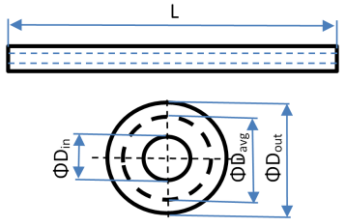


**Figure 2.** Geometry of the composite shaft used for the verification

The length (L) and average diameter ($d_{avg}$) of the composite shaft were 1.730 and 50.3 mm, respectively. The composite drive shaft was made of four E glass fiber/epoxy layers (EG-EP) with the stacking sequence of $[90_{EG\text{-}EP}/45_{EG\text{-}EP}/\text{-}45_{EG\text{-}EP}/0_{EG\text{-}EP}]$. The mechanical properties of the composite shafts were given in Table 1. Each layer had a thickness of 0.6 mm. FE model was created by using 86,552 SOLID 185 elements with 108,500 nodes. Figure 3 shows the first mode natural frequency value and its mode shape. The first mode natural frequency was determined as 57.81 Hz. The difference between the calculated and reported value (57.61 Hz) was less than 1%. The torsional buckling of the hybrid $[45_{EG\text{-}EP}/\text{-}45_{EG\text{-}EP}/0_{CF\text{-}EP}/90_{EG\text{-}EP}]$ composite shafts were also determined in order to verify the finite element model for torsional buckling simulations. Figure 4 shows the first torsional buckling load and its corresponding eigenvalue.

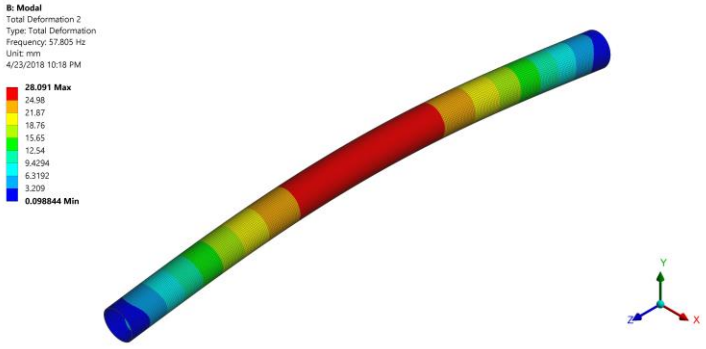


**Figure 3.** The first mode shapes of the composite shaft and its corresponding frequency value

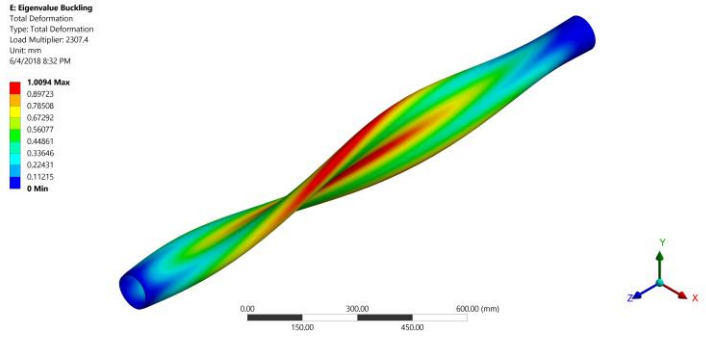


**Figure 4.** The first torsional buckling load of the composite and its corresponding buckling value

The torsional buckling load of the hybrid composite shaft was determined as 2307.4 N.m. The difference between the calculated and reported value (2327 N.m) was less than 1%. The validated FE model was extended to the current study.

## 2.2. Finite element modeling of PA 66 nanofiber interleaved composite shafts

In the composite shafts with PA 66 nanofiber interlayers, one PA 66 nanofiber interlayer (NFI) was placed between each EG-EP layer. Two different fiber orientations were considered; namely [45/NFI/-45/NFI/0/NFI/90] and [0/NFI/90/NFI/0/NFI/90]. The length and inner diameter of the composite shaft were 1730 and 99.2 mm, respectively. Each layer had a thickness of 0.6 mm. Three different nanofiber areal weight densities, 8, 10 and 12 g/m$^2$, were considered in the nano-modified composites. The NFI thickness for 8, 10 and 12 g/m$^2$ was 70, 85, 100 μm, respectively. Table 1 shows the physical and mechanical properties of E glass/epoxy layer (EG-EP), carbon fiber/epoxy layer (CF-EP) and PA 66 nanofiber interlayers. The material constants of the PA 66 NFI were calculated according to the rule of mixture. A more detailed explanation about the calculation material constants of nanointerlayers can be found in Reference [13]. Figure 5 shows finite element model of the reference and nanomodified composite shafts and applied boundary and loading conditions for free-vibration and torsional buckling analysis. In total, 86,522 and 151,466 SOLID185 elements were used to create 3D FE model of reference and nanomodified composite shafts,

respectively. One element was used for each ply through the thickness of composite shaft.

**Table 1**. Mechanical and physical properties of E glass/epoxy composite and PA 66 nanofiber interlayers [10, 11].

| | EG/ EP [11] | CF/ EP [11] | PA 66 NFI [10] |
|---|---|---|---|
| $E_1$(GPa) | 40.3 | 126.9 | 3.0 |
| $E_2$(GPa) | 6.21 | 11.0 | 0.75 |
| $G_{12}$ (GPa) | 3.07 | 6.6 | 0.80 |
| $\upsilon_{12}$(-) | 0.20 | 0.28 | 0.35 |
| $\rho$ (kg/m$^3$) | 1910 | 1610 | 1140 |

## 3. Results

Table 2 shows the values of first five natural frequencies of reference and PA 66 nanomodified composite shafts having a fiber sequence of [45/NFI/-45/NFI/0/NFI/90]. A negligible decrease about 2.3% was observed for the first and second natural frequency values with the addition of PA 66 nanofiber interlayers. As expected, the less stiff PA66 nanofibers in the interlaminar region caused a small reduction in the values of first and second natural frequencies. On the other hand, the third, fourth and fifth natural frequencies showed a slight increase as a result of the incorporation of nanofibers into the composite shafts. The frequency values increased by 10.5% after the addition of 12 gsm PA66 nanointerlayers. These results were consistent with the results of Garcia et al. [10]. Another important observation was that there is almost linear relationship between the natural frequency values and the amount of nanofibers in the interlaminar region. The increase in AWD led to higher improvement in the natural frequency values.

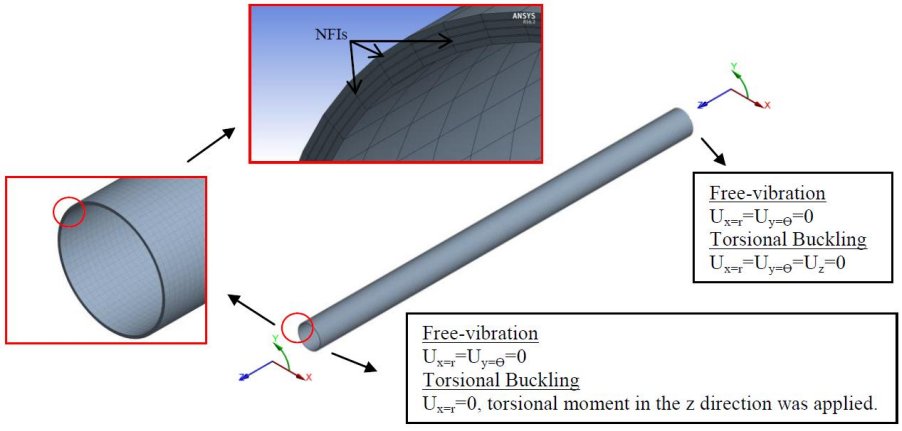


**Figure 5.** Finite element model of nanomodified composite shaft and boundary/loading conditions

**Table 2**. The natural frequency values of the reference and PA 66 nanointerlayer composite shafts (Lamination sequence:[45/NFI/-45/NFI/0/NFI/90])

| Composite shaft | 1st mode (Hz) | 2nd mode (Hz) | 3rd mode (Hz) | 4th mode (Hz) | 5th mode (Hz) |
|---|---|---|---|---|---|
| Reference | 57.2 | 221.6 | 377.7 | 388.8 | 393.3 |
| PA 66 AWD-8.0 gsm | 56.3 | 217.9 | 405.7 | 417.2 | 422.4 |
| PA 66 AWD-10.0 gsm | 56.1 | 217.2 | 411.6 | 423.1 | 428.5 |
| PA 66 AWD-12.0 gsm | 55.9 | 216.5 | 417.3 | 428.9 | 434.5 |

**Table 3**. The natural frequency values of the reference and PA 66 nanointerlayer composite shafts (Lamination sequence:[0/NFI/90/NFI/0/NFI/90])

| Composite shaft | 1st mode (Hz) | 2nd mode (Hz) | 3rd mode (Hz) | 4th mode (Hz) | 5th mode (Hz) |
|---|---|---|---|---|---|
| Reference | 63.3 | 232.3 | 366.4 | 379.0 | 386.3 |
| PA 66 AWD-8.0 gsm | 62.2 | 228.3 | 361.2 | 406.5 | 413.1 |
| PA 66 AWD-10.0 gsm | 61.9 | 227.4 | 360.2 | 412.2 | 418.6 |
| PA 66 AWD-12.0 gsm | 61.7 | 226.6 | 359.2 | 417.9 | 424.2 |

The first torsional buckling mode and its corresponding buckling torque of reference and PA 66 nanointerlayed composite shafts were shown in Figure 6.

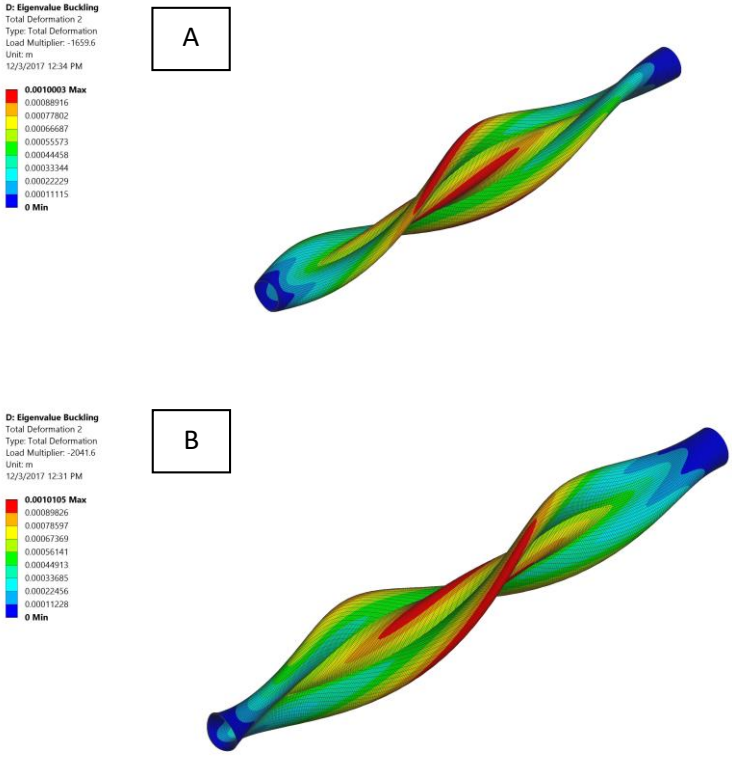


**Figure 6.** The first torsional buckling mode and its corresponding buckling torque of (a) reference and (b) nanomodified composite shaft (Lamination sequence:[0/NFI/90/NFI/0/NFI/90])

Table 3 shows the values of first five natural frequencies of reference and PA 66 nanomodified composite shafts having a fiber sequence of [0/90/0/90]. The reference composites had a higher 1st and 2nd mode natural frequency values compared to [45/-45/0/90] composites. This can be explained by the increase in $D_{11}$ values (GPa.mm) due to fiber orientation. The bending stifness matrices of the composite shafts were given in Equations (1) and (2). As in the of

[45/-45/0/90] fiber orientation, a negligible decrease about 2.5% was observed for the first and second natural frequency values with the addition of PA 66 nanofiber interlayers. On the other hand, the fourth and fifth natural frequencies showed a slight increase as a result of the incorporation of nanofibers into the composite shafts. The frequency values increased about 10% after the addition of 12 gsm PA66 nanointerlayers.

$$D_{[45/-45/0/90]} = \begin{bmatrix} 14.94 & 6.050 & 3.705 \\ 6.050 & 29.75 & 3.705 \\ 3.705 & 3.705 & 8.147 \end{bmatrix} \quad (1)$$

$$D_{[0/90/0/90]} = \begin{bmatrix} 26.96 & 1.440 & 0 \\ 1.440 & 26.96 & 0 \\ 0 & 0 & 3.537 \end{bmatrix} \quad (2)$$

Table 4 shows the critical torsional buckling loads of reference and nanomodified composite shafts. The critical buckling load for the reference composites having [45/NFI/-45/NFI/0/NFI/90] fiber orientation were determined as 1659.6 N. The addition of PA 66 nanointerlayers improved critical buckling loads significantly. Almost 23% increase was obtained with the inclusion of PA 66 nanofibers with an AWD value of 12.0 gsm. As observed in the natural frequency analyses, there is a linear relationship between buckling load and the amount of nanofibers in the interlaminar region. Table 4 also shows the torsional buckling loads of the composite shafts having [0/90/0/90] fiber orientation. As can be seen, the torsional buckling loads were higher than those of the composites having [45/-45/0/90]. This can be explained by the variation in the extensional stiffness matrix values ($A$, GPa-mm$^3$) due to the change of fiber orientation. It is known that the stiffness modulus in hoop direction which direclty related to the extensional stiffness matrix plays the most substantial role in increasing the buckling resistance. The extensional stiffness (A) of the reference composite shafts were given in Equations (3) and (4).

$$A_{[45/-45/0/90]} = \begin{bmatrix} 46.55 & 12.61 & 0 \\ 12.61 & 46.55 & 0 \\ 0 & 0 & 16.97 \end{bmatrix} \quad (3)$$

$$A_{[0/90/0/90]} = \begin{bmatrix} 56.16 & 2.999 & 0 \\ 2.999 & 56.16 & 0 \\ 0 & 0 & 7.368 \end{bmatrix} \quad (4)$$

As in the case of the composite shafts having[45/NFI/-45/NFI/0/NFI/90] fiber orientation, the addition of PA 66 nanointerlayers improved critical buckling loads significantly. A 22% increase was obtained with the inclusion of PA 66 nanofibers with an AWD value of 12.0 gsm. As observed in the natural frequency analyses, there is a linear relationship between buckling load and the amount of nanofibers in the interlaminar region.

Table 4 shows the failure torque of the composite shafts. In order to determine failure torque of the composite shafts, a torque with a magnitude of 1500 N. m was applied to the left-end of the composite shaft and the failure indices were evalauted for each ply using ANSYS ACP-Post Module. The failure torque was calculated by dividing applied torque by the maximum Tsai-Wu failure index.

**Table 4**. Torsional buckling loads and torsional capacity of the composite shafts

| Composite shaft [45/NFI/-45/NFI/0/NFI/90] | Torsional buckling load (N.m)/Failure torque (N.m) |
|---|---|
| Reference | 1659.6/2245 |
| PA 66 AWD-8.0 gsm | 1923.6/2276 |
| PA 66 AWD-10.0 gsm | 1982.2/2287 |
| PA 66 AWD-12.0 gsm | 2041.6/2298 |
| Composite shaft [0/NFI/90/NFI/0/NFI/90] | Torsional buckling load (N.m)/Failure torque (N.m) |
| Reference | 2105.2/3035.8 |
| PA 66 AWD-8.0 gsm | 2425.2/3113.3 |
| PA 66 AWD-10.0 gsm | 2495.8/3129.6 |
| PA 66 AWD-12.0 gsm | 2567.2/3145.3 |

The maximum Tsai-Wu failure indices were determined as 0.668, 0.659, 0.656, and 0.6527 for reference, PA 66 modified AWD-8.0 gsm, PA 66 modified AWD-10.0 gsm, PA 66 modified AWD-12.0 gsm interleaved composites having [45/NFI/-45/NFI/0/NFI/90] fiber orientation, respectively. Although a small increase was observed in failure torques after the addition of PA 66 nanofibers, it can be said that the failure torque values were not significantly affected by these nanofibers.

For the composite shafts with [45/NFI/-45/NFI/0/NFI/90] fiber orientation, the maximum Tsai-Wu failure indices were determined as 0.494, 0.481, 0.479, and 0.476 for reference, PA 66 modified AWD-8.0 gsm, PA 66 modified AWD-10.0 gsm, PA 66 modified AWD-12.0 gsm interleaved composites, respectively. A small increase (about 3.5%) was observed in failure torques after the addition of PA 66 12 gsm nanofibers. As in the case of [45/NFI/-45/NFI/0/NFI/90] fiber orientation, the failure torque values were not affected by these nanofibers.

## 4. Discussion and Conclusion

In this study, numerical analyses were carried out to investigate the effects of PA 66 nanointerlayers on the free vibration (the first five natural frequency values), critical torsional buckling load and failure torque of E glass/epoxy composite drive shafts. The aim was to investigate the potential use of these nanointerlayers in composite drive shafts. The numerical model of the composite shaft was created by using ANSYS Workbench (ACP Module) and verified on the basis of the results from the literature. The conclusions were summarized as follows:

•The 1st and 2nd mode natural frequency values decreased due to the integration of less stiff PA nanofibers between the primary E glass/epoxy plies. On the other hand, an increasing trend was observed for 3rd, 4th and 5th natural frequency values.

•The natural frequencies of the composite shaft can be increased by about 10 % using PA 66 nanofibers as the secondary reinforcing material in the interlaminar region.

•The critical torsional buckling load of the composite shaft increased in the range of 22-23% after the incorporation of PA 66 nanofibers.

•There is almost a linear relationship between the natural frequencies, buckling loads and the amount of nanofibers in the interlaminar region.

•The failure torque values were not significantly affected with the inclusion of PA 66 nanofibers.

## References

[1] Greenhalgh, E.S., Rogers, C., Robinson, P. 2009. Fractographic observations on delamination growth and the subsequent migration through the laminate. Composites Science and

Technology, Cilt. 69(14), s. 2345-2351.DOI:10.1016/j.compscitech.2009.01.034

[2] Greenhalgh E.S. 2009. Failure analysis and fractography of polymer composites, CRC Press.

[3] Beylergil, B., Tanoglu, M., Aktaş, E. 2017. Enhancement of interlaminar fracture toughness of carbon fiber/epoxy composites using polyamide 6/6 electrospun nanofibers. Journal of Applied Polymer Science, Cilt. 134(35): 45244. DOI: 10.1002/app.45244

[4] Daelemans, L., van der Heijden, S., De Baere I, Rahier H, Van Paepegem, W., De Clerck, K.2015. Nanofibre bridging as a toughening mechanism in carbon/epoxy composite laminates interleaved with electrospun polyamide nanofibrous veils. Composites Science and Technology, Cilt. 117, s.244–256. DOI: 10.1016/j.compscitech.2015.06.021

[5] Zhang, H., Bharti, A., Li, Z., Du, S., Bilotti, E., Peijs, T. 2015. Localized toughening of carbon/ epoxy laminates using dissolvable thermoplastic interleaves and electrospun fibres. Composites Part A: Applied Science and Manufacturing, Cilt. 79: s. 116–26 DOI:10.1016/j.compositesa.2015.09.024

[6] Li, G., Li, P., Yu, Y., Jia, X., Zhang, S., Yang, X., Ryu, S. 2008. Novel carbon fiber/epoxy composite toughened by electrospun polysulfone nanofibers. Materials Letters, Cilt.62(3), s. 511–514. DOI: 10.1016/j.matlet.2007.05.080

[7] Li, G., Li, P., Zhang, C., Yu, Y., Liu, H., Zhang, S., Jia, X., Yang, X., Xue, Z., Ryu, S. 2008. Inhomogeneous toughening of carbon fiber/epoxy composite using electrospun polysulfone nanofibrous membranes by in situ phase separation. Composites Science Technology Cilt.68(3–4)i s. 987–94. DOI: 10.1016/j.compscitech.2007.07.010

[8] Saghafi, H., Brugo, T., Minak, G., Zucchelli, A. 2015. The effect of PVDF nanofibers on mode-I fracture toughness of composite materials. Composites Part B: Engineering, Cilt.72, s. 213–216. DOI:10.1016/j.compositesb.2014.12.015

[9] Beckermann, G.W. 2017. Nanofiber interleaving veils for improving the performance of composite laminates. Reinforced Plastics, Cilt. 61(5), s. 289-93. DOI: 10.1016/j.repl.2017.03.006

[10] Garcia, C., Wilson, J., Trendafilova, I., Yang, L. 2017. Vibratory behaviour of glass fibre reinforced polymer (GFRP) interleaved with nylon nanofibers. Composite Structures, Cilt. 176, s. 923–932. DOI: 10.1016/j.compstruct.2017.06.018

[11] Khalkhali, A., Nikghalb, E., Norouzian, M. 2015. Multi-objective optimization of hybrid carbon/glass fiber reinforced epoxy composite automotive drive shaft. Int. J. Eng, Cilt. 28(4), s.583–592.

[12] Talib, A.R.A, Ali, A., Badie, M.A., Lah, N.A.C, Golestaneh, A.F. 2010. Developing a hybrid, carbon/glass fiber-reinforced, epoxy composite automotive drive shaft, Materials and Design, Cilt. 31, s. 514-521. DOI:10.1016/j.matdes.2009.06.015.

[13] Zhu, P., Lei, Z.X., Liew, K.M. 2012. Static and free vibration analyses of carbon nanotubereinforced composite plates using finite element method with first order shear deformation plate theory. Composite Structures Cilt. 94, s. 1450-1460. DOI:10.1016/j.compstruct.2011.11.010.